Measurement of Lysozyme−Lysozyme Interactions with Quantitative Affinity Chromatography

Christopher A. Teske, Harvey W. Blanch, and John M. Prausnitz*

Department of Chemical Engineering, University of California-Berkeley and Chemical Sciences Division, Lawrence Berkeley National Laboratory, Berkeley, California 94720

Received: July 23, 2003; In Final Form: January 5, 2004

A chromatographic method is used to measure lysozyme−lysozyme interactions in aqueous salt solutions as a function of solution conditions (pH, ionic strength, and salt type). Compared to static light scattering and membrane osmometry, the chromatographic method requires significantly less protein. To interpret retention-time data, it is necessary to account for multibody interactions between a mobile lysozyme molecule and immobilized lysozyme molecules on the support surface. The interaction between lysozyme molecules may be described by a potential of mean force that contains hard-sphere, electrostatic, and square-well contributions. Square-well depths from chromatographic data are in semiquantitative agreement with those from osmotic second virial coefficients from static light scattering measurements.

Introduction

Quantitative data for protein−protein interactions provide useful information for the design of protein purification processes (e.g., salt-induced protein precipitation) and for determining solution conditions that favor formation of protein crystals that are required for X-ray diffraction studies to determine protein structure. A quantitative understanding of how solution conditions (pH, salt concentration, salt type, and temperature) influence protein−protein interactions is necessary for optimization of protein-separation processes. Further, attractive protein−protein interactions may result in protein precipitation, aggregation, or fibril formation, as observed in Alzheimer's,[1] Parkinson's,[2] and Huntington's diseases.[3]

Static and dynamic light scattering, ultracentrifugation, and membrane osmometry have been used to investigate protein−protein interactions. Results from these techniques are often expressed in terms of an osmotic second virial coefficient B_{22}, that is a measure of the net two-body protein−protein interaction in solution. However, both light scattering and osmometry suffer from the disadvantage of requiring a relatively large amount of protein (∼100 mg) for each desired solution condition. Further, with these methods it is difficult to measure interactions between different proteins because the second virial coefficient of individual proteins must be determined before making measurements on the mixture. Quantitative affinity chromatography provides a possible method to overcome both of these disadvantages.

Quantitative affinity chromatography is also known as analytical affinity chromatography,[4] self-interaction chromatography,[5] weak-affinity chromatography,[6] and affinity retardation chromatography.[7] Chromatography has been used to measure protein−ligand binding constants.[8] More recently, Patro et al.[5] and Tessier et al.[9] used chromatography to measure protein−protein interactions. Our work builds upon these recent significant studies.

We use quantitative affinity chromatography to measure lysozyme−lysozyme interactions at 25 °C as a function of pH, salt type, and ionic strength. Lysozyme was chosen as a model system because static light scattering (SLS) and osmometry data are available in the literature for comparison.[10−12]

Tessier et al.[9] studied lysozyme−lysozyme interactions using chromatography. Our work differs from that of Tessier et al. because we use much lower protein surface coverage. The lower protein concentration on the stationary phase allowed us to obtain concentration-independent retention volumes in the limit of low mobile-phase protein concentrations. Tessier et al. were unable to obtain concentration-independent retention volumes at low mobile-phase protein concentrations, possibly due to strong interaction "sites" on the stationary phase where one mobile protein can interact with many immobile proteins simultaneously. However, even with our low stationary-phase protein concentration, deviations between the chromatographic data obtained here and literature data for lysozyme−lysozyme interactions demonstrate the need to account for multibody interactions when interpreting chromatographic data. We present a simple model which allows us to account for multibody interactions. When we do so, comparison with results from light scattering is much improved.

Theoretical Framework

Chromatography with a Linear Adsorption Isotherm. For operating conditions where the adsorption isotherm is linear, the average retention volume becomes independent of the inlet pulse concentration in the mobile phase. The average retention volume of the mobile protein $\bar{V}_r$ is given by:[4]

$$\bar{V}_r = \bar{V}_0 + m_{ad}\left(\frac{d\bar{q}}{dc}\right)_{c\to 0} \quad (1)$$

where m_{ad} is the total mass of adsorbent in the column and $\bar{V}_0$ is the average retention volume of a noninteracting aqueous solute whose molecular size is close to that of the protein molecule. In our experiments, $\bar{V}_0$ is measured by injecting a pulse of protein onto a column under the same mobile-phase conditions used to determine $\bar{V}_r$, but containing no protein immobilized on the stationary phase. The derivative $(d\bar{q}/dc)_{c\to 0}$

* E-mail: prausnit@cchem.berkeley.edu.

10.1021/jp0361576 CCC: $27.50
Published on Web 05/12/2004

is the dilute-limit slope of the equilibrium isotherm that describes $\bar{q}$, the amount of protein adsorbed per mass of adsorbent, as a function of mobile-phase concentration, c. Experimentally, two pulses of low, but different protein concentration are injected at a given condition to verify that the experiments are conducted in the linear region of the adsorption isotherm.

To relate the slope of the isotherm at low protein concentrations to the potential of mean force between protein molecules, we use the adsorption virial equation[13] that gives $\bar{q}$ as a power series in c:

$$\bar{q} = Kc + ... \tag{2}$$

where K is a distribution factor.[14] K is also known as the adsorption second virial coefficient in the adsorption virial equation. We neglect higher-order terms in eq 2 because we are using low mobile-phase protein concentration. K provides a measure of the interaction between one mobile protein molecule and the stationary phase that includes immobilized proteins. By comparing eqs 1 and 2, we can relate the distribution factor to the retention data in the limit of low mobile-phase protein concentration:

$$K = \frac{\bar{V}_r - \bar{V}_0}{m_{ad}} \tag{3}$$

The distribution factor is related to the potential of mean force between a mobile solute molecule and the stationary-phase surface,[13,14] which includes immobile proteins:

$$K = \frac{1}{m_{ad}} \int_v [\exp(-w'(x, y, z)/kT) - 1]\, dx\, dy\, dz \tag{4}$$

where $w'(x, y, z)$ is the dilute solution potential of mean force between a single mobile protein molecule and the protein-loaded stationary-phase surface as a function of the molecule's position relative to the surface. Here v indicates that eq 4 is a volume integral over the entire mobile-phase volume. To relate our measurements to static light scattering and membrane osmometry measurements, we assume that all contributions to w' are only from interactions between a mobile protein and immobile proteins on the surface, i.e., we do not include in w' any interaction between the mobile protein and a bare (protein-free) stationary phase. We recognize that a mobile protein may interact with the bare surface that is free of immobile proteins; to account for any weak interactions that the mobile protein may have with the bare surface, the retention volume, $\bar{V}_r$, is measured relative to $\bar{V}_0$, the retention volume measured using a protein-free stationary phase. Thus, $\bar{q}$ represents the amount of mobile protein adsorbed beyond that adsorbed on a protein-free stationary phase. Figure 1 illustrates a mobile protein interacting with a stationary phase.

Chromatographic Determination of B_{22}. The osmotic second virial coefficient B_{22} reported from static light scattering and membrane osmometry experiments is rigorously related to the two-body potential of mean force between protein molecules in solution through the McMillan−Mayer solution theory:[15]

$$B_{22} = -2\pi \int_0^\infty [\exp(-w(r)/kT) - 1]\, r^2\, dr \tag{5}$$

where $w(r)$, the two-body potential of mean force, is defined as the work required to bring two infinitely separated protein molecules to a finite separation r, averaged over all possible configurations of the solvent molecules. Equation 5 assumes that the potential of mean force is spherically symmetric.

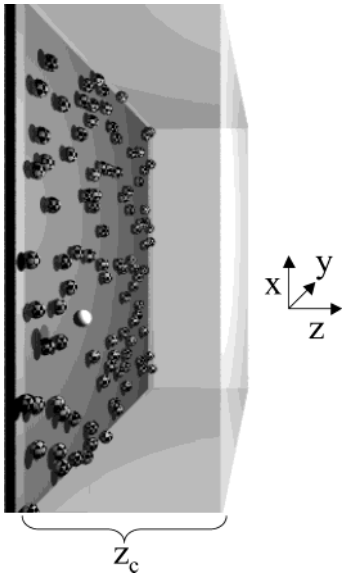

Figure 1. A three-dimensional representation of a mobile protein interacting with the stationary phase. A mobile lysozyme molecule (white) is located near the protein-loaded stationary-phase surface. $z = 0$ is the plane which passes through the centers of the immobilized protein molecules that are tangent to the planar surface. The distribution factor can be calculated using eq 4 evaluated over the shaded volume in the figure. Beyond the cutoff distance z_c, the value of the integrand in eq 4 is zero. The presence of the solid surface means that the mobile protein accesses only a hemispherical region of the potential around an isolated immobile protein. When a mobile protein approaches a region close to a cluster of immobilized proteins, w', the potential of mean force between a mobile lysozyme molecule and the lysozyme-loaded stationary phase contains contributions from interactions of the mobile protein with multiple immobile proteins. In that event, w' has a complex dependence on (x, y, z).

Equation 5 is similar to eq 4. However, $w'(x, y, z)$ is not necessarily the same as $w(r)$. In general, w' may contain contributions from the simultaneous interaction of a mobile-phase protein with several immobile proteins on the surface of the stationary phase, while $w(r)$ considers only a two-body protein−protein interaction. Further, the immobilized protein in our experiments has lost some of its rotational freedom. Thus, if w depends on orientation, w' differs from w. This effect is mitigated if the protein is immobilized in a variety of orientations such that, as a mobile protein travels through the column, it interacts with immobile proteins in a variety of orientations. The immobilization technique used in our experiments attaches proteins to the stationary phase through the primary amine groups of the lysine residues and the terminal amine. Other researchers[5,9] have assumed that this immobilization technique leads to random attachment of lysozyme to the surface. Determining the actual orientation distribution of lysozyme is an extremely difficult task. For our analysis, we assume that $w(r)$ is spherically symmetric as written in eq 5.

If the range of $w(r)$ is very short, much shorter than the average center-to-center spacing between immobilized molecules, then a given mobile-phase protein molecule only interacts with a single immobile protein molecule at a given position, i.e., $w' = w$ at every position, and the integral in eq 4 simplifies to:

$$K = 2\pi N \int_0^\infty [\exp(-w(r)/kT) - 1] r^2\, dr = -NB_{22} \tag{6}$$

where N is the number of accessible immobilized molecules in the column per mass of adsorbent. For our calculations, we assume that all immobilized lysozyme molecules are accessible

because of the large pore size of our stationary phase. On the basis of these assumptions, we calculate an apparent B_{22} from our chromatography experiments according to:

$$B_{22}^{app} = \frac{-K}{N} = \frac{\bar{V}_0 - \bar{V}_r}{m_{ad}N} \quad (7)$$

The product $m_{ad}N$ in the denominator represents the total number of accessible immobilized molecules, and thus it is not necessary to know m_{ad} to calculate B_{22}^{app}. However, it is important to note that eq 7 is for an ideal case, valid only when w is spherically symmetric and, more important, when the distance between immobilized molecules is large compared to the effective range of $w(r)$. At higher surface coverage, we expect B_{22}^{app} to differ from B_{22} as measured by static light scattering or membrane osmometry because in chromatography, a mobile protein interacts simultaneously with several immobilized molecules, as suggested in Figure 1. Because eq 7 is used to analyze data even at surface coverages where multibody interactions are important, we have added the superscript "app" to B_{22} to indicate an "apparent" second virial coefficient.

Equation 7 is similar to that developed by Tessier and coworkers,[9] relating their chromatographic data to protein−protein interactions. In their analysis, Tessier et al. include a separate excluded-volume contribution, calculated from the equivalent spherical diameter of the protein. They add this excluded-volume term to their chromatographic measurement to give their final value of B_{22}. However, in our analysis, the excluded-volume interaction is already captured in our experimental measurement because we measure a retention volume in excess of that for a protein-free stationary phase.

Multibody Interactions in Chromatography. To decide whether results from a particular affinity-chromatography experiment satisfy the assumptions implicit in eq 7, we need an estimate of the range of $w(r)$. Provided that the ionic strength of the solution gives sufficient screening, the largest contributions to protein interactions are short-ranged; these can be described by a square-well potential. A typical square-well width parameter for proteins is $\lambda = 1.2$[16,17] where $(\lambda - 1)$ is the reduced width of the square well. We assume that the stationary phase can be represented as a large planar surface. If the immobilized proteins are arranged on a square lattice on the surface of the stationary phase, we calculate the ratio of the center-to-center spacing L of adjacent protein molecules to the protein diameter σ from:

$$\frac{L}{\sigma} = \sqrt{\frac{\pi}{4\theta}} \quad (8)$$

where θ is the fractional surface coverage of immobilized protein. If L/σ is less than 2λ, a mobile protein molecule experiences the square-well potential of two adjacent immobilized molecules when it is positioned directly between them. Equation 8 predicts that this occurs at $\theta = 0.14$. This calculation is only meant to be a rough estimate of the surface coverage when multibody interactions will begin to occur. Tessier et al.[9] conducted experiments at $\theta = 0.33$; on the basis of our estimate, it is likely that multibody interactions occur in their experiments. We believe the value $\theta = 0.14$, in some cases, provides a high estimate of the fractional surface coverage when multibody interactions begin because it is based on a short-ranged square-well potential; electrostatic interactions between proteins at low-ionic strength are longer ranged than the square-well potential used here; further, immobilized protein molecules on the surface are probably not uniformly spaced. Thus, some multibody interactions are likely to occur at fractional surface coverage less than 0.14.

Previous analyses of chromatographic data for protein−protein interactions have implicitly assumed (as we have above in determining L) that the immobilized protein is uniformly spaced on the stationary-phase surface. However, even for a small protein like lysozyme, the stationary phases used in affinity chromatography typically have a large excess of potential immobilization sites (aldehyde groups in our case), implying that the ratio of immobilized proteins to sites is small even if the stationary-phase surface is at maximum coverage. Thus, when compared to the size of the protein, the spacing between potential immobilization sites is small; in effect, the surface provides a continuum of sites where a protein can be immobilized.

During immobilization of the protein, protein−protein interactions occur in solution. These interactions may lead to different structures of the immobilized protein layer, depending on the solution conditions that prevail during immobilization. Qualitatively, if there are strongly repulsive protein−protein interactions during immobilization, immobilized protein molecules tend to be widely spaced. However, strongly attractive protein−protein interactions during immobilization may produce protein clusters on the surface of the stationary phase. Finally, if the proteins behave as hard spheres, the immobilized layer will be organized consistently with random sequential adsorption.[18] In our method of data analysis, we consider the case when the immobilized protein molecules are randomly arranged on the surface of the stationary phase. An important feature of our analysis, when compared with the uniformly spaced model, is that we take into account the presence of protein clusters even at low surface coverage, because of the random nature of the immobilization process. These clusters serve as "sites" on the stationary phase where a mobile-phase protein interacts with two or more immobilized proteins.

Experimental Section

Materials. Hen egg white lysozyme (L-6876, 95% purity), periodate-activated agarose, and sodium cyanoborohydride were purchased from Sigma (St. Louis, MO). Salts (>99% purity) were purchased from Fisher (Los Angeles, CA). Fluorescein-isothiocyanate (FITC) was purchased from Molecular Probes, Inc. (Eugene, OR). All solutions were prepared using water obtained from a Barnstead Nanopure water system (Dubuque, IA).

Equipment. A lysozyme-loaded stationary phase was packed into a chromatography column of length 5 cm × 0.5 cm inner diameter. The column is part of a Pharmacia basic FPLC system. The system consists of a LCC-501 controller, 2 P-500 pumps, a UV−IIM detector, and an MV-7 injection valve, all controlled by a personal computer. pH values of buffer and salt solutions were measured using a Sargeant-Welch (8400) pH meter with a Beckman (39847) electrode. Protein concentrations were determined using a Shimadzu UV-160 spectrophotometer.

Lysozyme Immobilization. The immobilization of lysozyme to periodate-activated agarose was based on the method described by Domen et al.[19] Four milliliters of periodate-activated agarose was mixed with 4 mL of lysozyme-containing coupling buffer (5 mM sodium acetate at pH 4.5). Thirty-two milligrams of sodium cyanoborohydride was added to the mixture. The coupling reaction was allowed to proceed overnight at room temperature on a rotating mixer. The protein-loaded stationary phase was then washed on a sintered glass filter with 100 mL of the coupling solution, followed by 100 mL of 1M

NaCl, and then again with 100 mL of coupling solution to remove protein not covalently attached to the stationary phase. Wash solutions were collected and analyzed for remaining lysozyme by spectrophotometry using the extinction coefficient of lysozyme 2.63 mL/(mg cm) at 280 nm.[20] The mass of lysozyme in the wash solutions was subtracted from the amount in the coupling solution to give the amount of lysozyme immobilized on the stationary phase.

Preparation of Mobile-Phase Protein Samples. A lysozyme stock solution of approximately 5 mg/mL was prepared by dissolving lysozyme powder into the appropriate buffer. Solutions at pH 4 to 5 were buffered by 20 mM sodium acetate; solutions at pH 7 were buffered by 20 mM sodium phosphate. The lysozyme stock solution was filtered with a 0.2 μm syringe filter before the concentration of the stock solution was determined by absorbance at 280 nm as described above. Mobile-phase lysozyme samples were prepared by diluting the protein stock solution with the necessary volume of buffer and a 2.0 m concentrated solution of the appropriate salt in the same buffer.

Zonal Chromatography Experiments. A 25 μL pulse of dilute aqueous acetone (2% v/v) was injected to determine the extent of dispersion or channeling in the packed bed. If the exiting acetone peak was not symmetric, the column was repacked.

All chromatographic experiments were carried out at 25 °C. Preliminary data showed that our results were essentially independent of flow rate in the region tested (0.05−0.40 mL/min). We report results at a flow rate of 0.2 mL/min. Before data acquisition, the column was equilibrated with at least five column volumes of the same aqueous salt solution in which the subsequent experiment was performed. A run consisted of injecting a pulse of dilute buffered aqueous lysozyme and monitoring the absorbance at 280 nm at the column exit until all of the mobile lysozyme had emerged. Two lysozyme concentrations (0.12 and 0.25 mg/mL) were injected at each solution condition to verify that experiments were conducted in the linear region of the adsorption isotherm.

Analysis of Zonal Chromatography Data. Retention volumes were determined from chromatographic data using moment analysis.[21] The average retention volume is given by the first absolute moment $\bar{V}$:

$$\bar{V} = \frac{\int_0^\infty Vc\, dV}{\int_0^\infty c\, dV} \tag{9}$$

where c is the concentration of mobile protein exiting the column as a function of the volume, V, of aqueous salt solution that has passed through the column. V can be calculated by $V = Ft$ where F is flow rate and t is time. Both $\bar{V}_r$ and $\bar{V}_0$ were evaluated at each solution condition using eq 9.

Confocal Scanning Laser Microscopy Experiments. Confocal scanning laser microscopy was used to determine the concentration of immobilized lysozyme as a function of radial position in the support particles. Lysozyme (after immobilization on the stationary phase) was labeled with fluorosceinisothiocyanate (FITC) according to directions specified by the manufacturer. A large excess of dye molecules were present in solution to ensure uniform labeling of immobilized lysozyme. Confocal images were acquired with a Leica confocal scanning laser microscope using a 63× oil-immersion lens. An argon/krypton laser excited the fluoroscein at 488 nm; emitted light was detected at 515−540 nm. The focal plane passing through the middle of a stationary particle was found by varying the location of the focal plane until the cross-sectional area of particle in the image was a maximum. Analysis of the images for fluorescence intensity as a function of position was performed using software supplied by Leica.

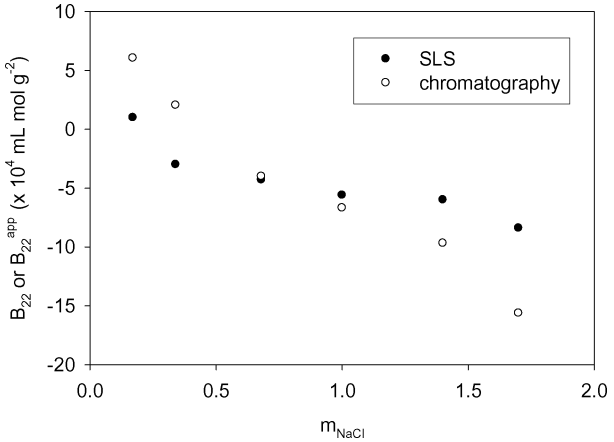

Figure 2. Comparison of B_{22}^{app} for lysozyme−lysozyme interactions in NaCl (pH 4.5, 25 °C) measured by chromatography in this work to values of B_{22} determined by static light scattering (SLS) by Curtis et al.[12]

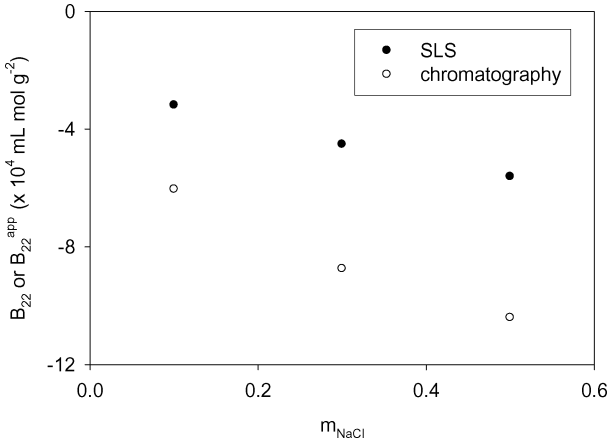

Figure 3. Comparison of B_{22}^{app} for lysozyme−lysozyme interactions in NaCl (pH 7.0, 25 °C) measured by chromatography in this work to B_{22} interpolated from the SLS results of Velev et al.[11]

Results and Discussion

Experimental Results. Figure 2 shows a comparison of B_{22}^{app} calculated from our chromatographic results using eq 7 and B_{22} measured by static light scattering at 25 °C and pH 4.5 as a function of sodium chloride concentration. The column contained a lysozyme-loaded stationary phase with approximately 10 mg of lysozyme/mL of packed bed volume. Lysozyme was immobilized to the stationary phase in 5 mM sodium acetate at pH 4.0, conditions where lysozyme−lysozyme interactions are weakly repulsive. Our measurements are independent of mobile-phase protein concentration provided that this concentration is small, below 0.25 mg/mL.

Results from light scattering and chromatographic experiments are qualitatively similar; both show increasing lysozyme−lysozyme attraction with increasing salt concentration. However, the chromatographic data show more repulsion at low ionic strengths and more attraction at high ionic strengths. Figures 3 and 4 compare B_{22}^{app} for lysozyme−lysozyme interactions measured with our chromatographic method with B_{22} values from

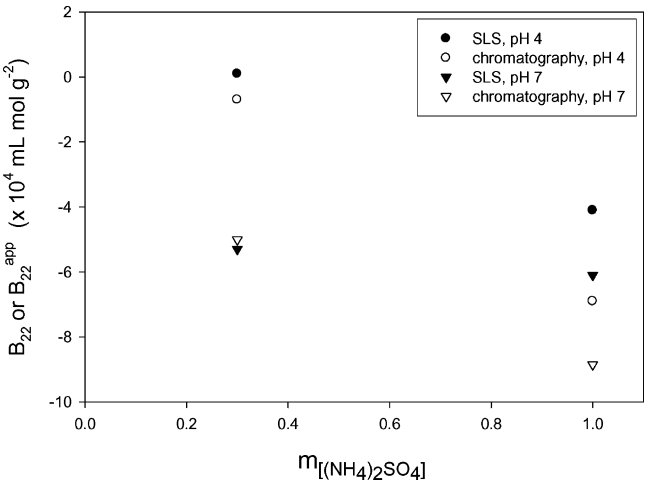

Figure 4. Comparison of B_{22}^{app} for lysozyme−lysozyme interactions in ammonium sulfate (pH 4.0 and 7.0, 25 °C) measured by chromatography in this work to the SLS measurements of Curtis et al.[12]

light scattering at various solution conditions. Both experimental methods show the same qualitative trends for lysozyme−lysozyme interactions: increasing attraction with increasing ionic strength. However, the chromatographic results are typically more attractive than those obtained by light scattering. Curtis et al.[12] report an experimental uncertainty in their B_{22} values of not more than 1×10^{-4} (mL mol g^{-2}); thus, the discrepancy between the light scattering and chromatographic results is not due to experimental error. We expect that this effect is due to simultaneous interaction of a mobile-phase molecule with two or more immobilized molecules.

Accounting for Multibody Interactions. Lysozyme Spacing on the Stationary-Phase Surface. To determine the average spacing between immobilized molecules, we required an estimate of the surface area of the stationary phase. This was obtained by experimentally determining the maximum amount of lysozyme that could be immobilized on the stationary phase and then calculating the total surface area, assuming that the lysozyme particles were in a hexagonally close-packed monolayer ($\theta = 0.91$) on the surface. We also used the model of Dephillips et al.[22] to calculate the surface area using 42 nm as the average pore size of Sepharose CL-4B.[23] Both methods gave surface areas in good agreement: 22 and 27 m^2/mL of mobile-phase volume, respectively. Thus, our experiments were performed at $\theta = 0.14$ or 0.17, depending on which estimate of the surface area was used.

Organization of Immobilized Lysozyme. The organization of immobilized lysozyme on the surface of the stationary phase is expected to influence how a mobile molecule interacts with the stationary phase. Qualitatively, if immobile protein molecules are organized in large clusters, we expect that mobile-phase lysozyme will interact very strongly with these clusters under conditions where lysozyme−lysozyme interactions are attractive. For simplicity, we neglect the complex structure of the stationary-phase pores and model the stationary phase as a large planar surface. The actual organization of immobilized lysozyme molecules on the surface will depend on lysozyme transport from bulk solution to the surface, the rate of protein surface diffusion, and the kinetics of the immobilization reaction. Several recent theoretical studies have explored the ordering of adsorbed proteins on surfaces.[24,25] Here we consider only lysozyme molecules randomly organized on the surface of the stationary phase.

Monte Carlo simulations were carried out to generate a representation of lysozyme immobilized on our stationary phase. The locations of immobilized lysozyme molecules on the surface are generated through random sequential adsorption to the surface. Lysozyme was assumed to be a sphere of diameter 3.44 nm. All surfaces were 100 nm × 100 nm with periodic boundary conditions. All immobilized molecules were assumed to be tangent to the planar surface. To generate a surface of randomly placed lysozyme molecules, a point was chosen at random on the surface, and the coordinates of this point became the location of the center of the first immobilized molecule. Further locations were determined by picking another point at random and checking to see if a newly placed molecule at that location overlaps with any previously placed molecules. If overlap occurs, placement of a molecule at that point was rejected and a new point was randomly chosen. This process was repeated until the necessary surface coverage was reached. Figure 5 shows representative surfaces at different surface coverage. It is evident that lysozyme molecules are not arranged in a regular geometric pattern. Significant numbers of lysozyme clusters are present at all surface coverages shown.

A Model for the Lysozyme−Lysozyme Potential-of-Mean-Force. To calculate the effect of multibody interactions on the chromatographic results, we require the potential of mean force $w(r)$. Typically, the potential of mean force is modeled as a sum of contributions from DLVO theory, which includes hard sphere, electrostatic, and dispersion contributions, plus an additional contribution which accounts for specific interactions between proteins. Here we use a potential of mean force (eq 10) that includes contributions from hard-sphere repulsion (eqs 11 and 12), electrostatic repulsion (eq 13), and an attractive square-well potential (eq 14).

$$w_{tot}(r) = w_{hs}(r) + w_{elec}(r) + w_{sw}(r) \tag{10}$$

$$w_{hs}(r) = \infty \text{ for } r \le \sigma \tag{11}$$

$$w_{hs}(r) = 0 \text{ for } r > \sigma \tag{12}$$

$$w_{elec}(r) = kTD\frac{\exp(-\kappa r)}{r} \text{ for } r > \sigma \tag{13}$$

$$w_{sw}(r) = -\epsilon_{sw} \text{ for } \sigma \le r \le \lambda\sigma \tag{14}$$

where $D = z_p^2 L_B \exp(\kappa\sigma)/(1 + \kappa\sigma/2)^2$ with the Bjerrum length $L_B = e^2/(4\pi\epsilon_0\epsilon_r kT)$. The Debye screening length is κ^{-1} where $\kappa^2 = 8\pi L_B N_A I$, k is Boltzmann's constant, T is the temperature, z_p is the protein net charge, e is the elementary charge, $\epsilon_0\epsilon_r$ is the dielectric permittivity of the solvent, N_A is Avogadro's number, I is the ionic strength, and ϵ_{sw} and λ are the square-well depth and width parameters, respectively. We have not included an attractive dispersion-force contribution to avoid the complication of choosing a cutoff distance due to the divergence of the dispersion potential at contact. Thus, the square-well potential effectively includes a contribution from dispersion forces. Data for the protein net charge z_p as a function of pH were taken from Kuehner et al.[26]

Computation of the Distribution Factor. The distribution factor was calculated for a mobile lysozyme molecule interacting with a lysozyme-loaded stationary phase by evaluating eq 4 using Monte Carlo integration.[27] Periodic boundary conditions were used. We evaluated the integral in eq 4 by choosing a random point (x_i, y_i, z_i) from the mobile-phase volume. The plane $z = 0$, where z is coordinate perpendicular to the surface, is defined as the plane that passes through the centers of the immobilized molecules. The potential of mean force between

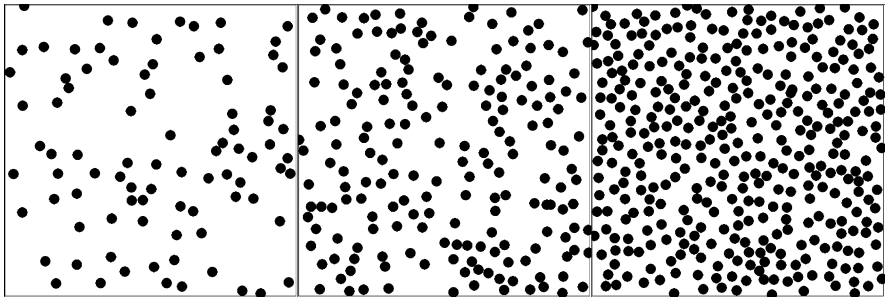

Figure 5. Representative surfaces generated from Monte Carlo simulations for lysozyme randomly immobilized at different fractional surface coverage θ. These surfaces correspond (from left to right) to $\theta = 0.085$, 0.17, and 0.33.

the mobile molecule and each immobile protein on the surface was determined by calculating the center-to-center distance between the mobile protein and the nearest image (due to periodic boundary conditions) of the respective immobile protein on the surface and applying eq 10. The total potential of mean force between the mobile molecule and the protein-loaded stationary phase is the sum of all two-body potentials between the mobile protein and all immobile proteins on the surface:

$$w'(x_i, y_i, z_i) = \sum_{i=1}^{N_{\text{immob}}} w_{\text{tot}}(r_i) \qquad (15)$$

where N_{immob} is the total number of immobilized molecules on the planar surface. The integrand in eq 4 can then be evaluated at that randomly chosen point. In principle, the integration is carried out over the total mobile-phase volume available to a mobile protein. However, in practice, only at positions close to the surface is there a nonzero contribution to the integral in eq 4. Thus, we do not need to consider points with $z > z_c$, where z_c is the cutoff distance. An appropriate value of z_c was determined by increasing z_c until the value of K no longer changed. We used $z_c = 3\sigma$ where σ is the diameter of lysozyme. The integral was calculated from

$$m_{\text{ad}}K = \frac{z_c A_s}{N_{\text{pts}}} \sum_{i=1}^{N_{\text{pts}}} \{\exp[-w'(x_i, y_i, z_i)/kT] - 1\} \qquad (16)$$

where A_s is the area of the planar surface and N_{pts} is the number of points at which the integrand is evaluated. The value of N_{pts} necessary to converge the integral to the desired precision was evaluated by trial and error. We used $N_{\text{pts}} = 10^6$.

Computed Effect of θ on B^{app}_{22}. Calculated distribution factors are presented in terms of predicted B_{22}^{app} values that are calculated by dividing the computed distribution factor by the total number of immobilized molecules N_{immob} according to eq 7. Figure 6 shows the effect of surface coverage on the predicted value of B_{22}^{app} for randomly placed immobile lysozyme molecules as a function of surface coverage using ϵ_{sw} values regressed from the static light scattering data of Curtis et al.[12] for $\lambda = 1.2$, which has been suggested to be typical for aqueous protein systems.[16,17] The calculations shown in Figure 6 were averaged over three different independently generated surfaces (locations of immobilized lysozyme molecules) at each surface coverage. When the net lysozyme−lysozyme interactions are weakly repulsive, the model predicts that B_{22}^{app} agrees well with B_{22} values. When lysozyme−lysozyme interactions are attractive, B_{22}^{app} becomes more negative (shows more attraction) than B_{22} as surface coverage is increased because of the interaction of a mobile-phase molecule with an increasing number of immobile protein clusters on the surface.

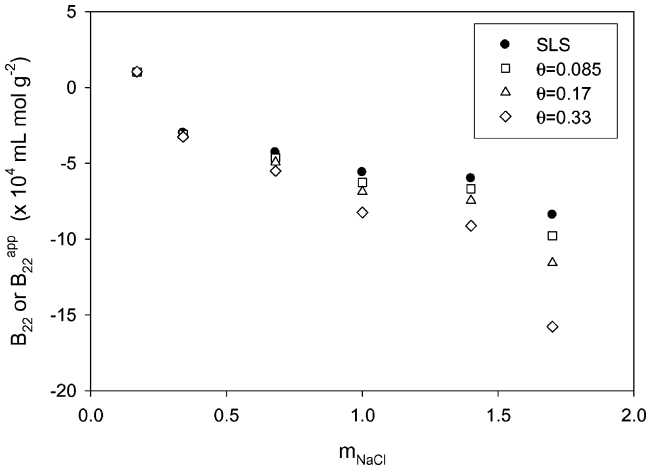

Figure 6. Calculated effect of fractional surface coverage θ on the predicted value of B_{22}^{app} according to our model accounting for multibody interactions. These results are for randomly immobilized molecules with square-well depths fit to the SLS results of Curtis et al.[12] at pH 4.5 using $\lambda = 1.2$. Also shown are the corresponding B_{22} from SLS.

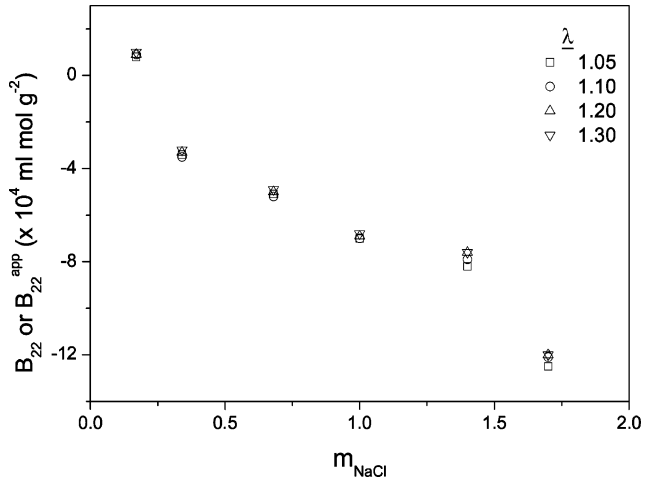

Figure 7. Effect of λ on the calculated value of B_{22}^{app} for $\theta = 0.17$. The ϵ_{sw} values used in the calculation were regressed from the SLS results of Curtis et al.[12] at pH 4.5.

Calculations were also performed to determine the sensitivity of the computed B_{22}^{app} to the choice of λ. Square-well depths were regressed from the light scattering data of Curtis et al.[12] for several values of λ and were then used in the calculation of B_{22}^{app}. Figure 7 demonstrates that the computed value of B_{22}^{app} is relatively insensitive to the choice of λ. $\lambda = 1.2$ was used for the rest of the calculations in our study.

Table 1 shows the best-fit value of ϵ_{sw} from our chromatographic data, determined for each solution condition, along with

TABLE 1: Best-Fit Values of the Square-Well Depth ϵ_{sw} for Lysozyme−Lysozyme Interactions to the Chromatographic Experiments after Accounting for Multibody Interactions, and the Corresponding Values of ϵ_{sw} from Static Light Scattering (SLS) Measurements Fit to the Same Potential of Mean Force; $T = 298$ K

pH	salt	ϵ_{sw}/kT (chrom)	ϵ_{sw}/kT (SLS)
4.5	0.17 m NaCl	0.00	2.01
	0.34	0.90	1.96
	0.68	1.71	1.79
	1.00	1.82	1.83
	1.40	1.93	1.81
	1.70	2.11	1.99
7.0	0.1 m NaCl	2.73	2.57
	0.3	2.15	1.94
	0.5	2.06	1.88
4.0	0.3 m $(NH_4)_2SO_4$	1.25	1.07
	1.0	1.70	1.56
7.0	0.3 m $(NH_4)_2SO_4$	1.66	1.74
	1.0	1.80	1.74

ϵ_{sw} fit to the osmotic second virial coefficient data of Curtis et al.[12] and Velev et al.[11] using the same potential of mean force. Figure 8 shows a comparison of our experimental data with the model using our higher estimate of 17% surface coverage. The model semiquantitatively explains the discrepancy between the static light scattering data and our chromatographic data under attractive conditions; however, the model is unable to capture the greater repulsion of the chromatographic results at low ionic strength. Under attractive conditions, the square-well depths regressed from the chromatographic data are significantly greater than those from light scattering data. Slow pore diffusion of lysozyme during immobilization or radial variations in the concentration of potential immobilization sites may result in higher concentrations of immobilized lysozyme at the outside of the particle than in the center, leading to a higher effective surface coverage. For the attractive region of $w(r)$, the model data at 33% coverage (shown in Figure 6) using the square-well depth regressed from light scattering data agree very well with chromatographic data at 17% coverage. However, the model is not able to capture the extra repulsion at low ionic strengths.

Radial Variation in the Concentration of Immobilized Lysozyme. Confocal scanning laser microscopy (CSLM) provides a powerful tool to study the adsorption of proteins to porous stationary phases.[28,29] A lysozyme-loaded stationary phase was examined to determine the radial distribution of immobilized lysozyme. Figure 9 shows the fluorescence intensity as a function of the radial position in the particle. Although we have not yet ruled out fluorescence intensity variation due to the inner filter effect in this preliminary experiment, Figure 9 suggests that the concentration of lysozyme at the edge of the particle is roughly 2.5 times greater than that in the center. This implies a higher effective surface coverage that may partially account for the discrepancy between the square-well depths obtained from our chromatographic data and those from static light scattering data.

Relation of the Present Study to Previous Studies. Tessier and co-workers also studied lysozyme−lysozyme interactions using chromatography.[9] At a mobile-phase protein concentration of 1 mg/mL, concentration-independent retention volumes could not be obtained with a high surface coverage ($\theta = 0.33$) stationary phase. However, Tessier et al. found that at relatively high injection concentrations (~20 mg/mL) the retention volume became constant. This result was attributed to the presence of a small number of high-energy sites on the protein-loaded stationary phase where one mobile protein could interact

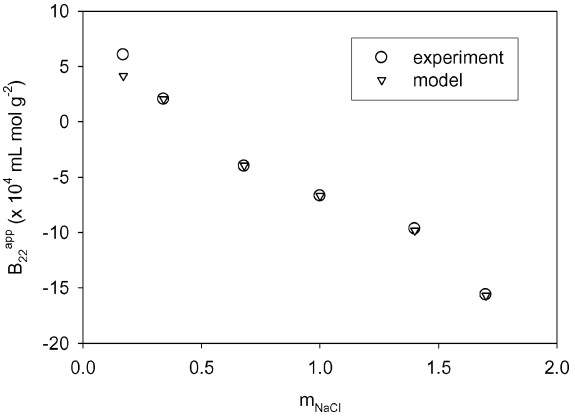

Figure 8. Comparison of experimental B_{22}^{app} (at pH 4.5) to model data accounting for multibody interactions at 17% surface coverage using ϵ_{sw} as a fitting parameter ($\lambda = 1.2$).

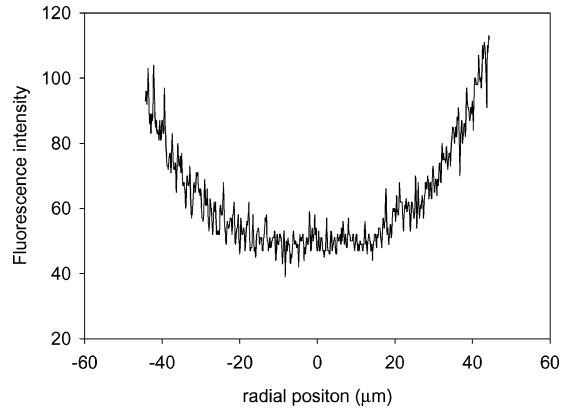

Figure 9. Fluorescence intensity as a function of position in a representative stationary-phase particle determined using confocal scanning laser microscopy. The immobilized lysozyme on the lysozyme-loaded stationary phase was labeled with fluorescein. The fluorescence intensity is not constant throughout the porous support particle; the data suggest that the immobilized lysozyme concentration varies with the radial position in a stationary-phase particle.

simultaneously with multiple immobilized proteins. Tessier et al. claim that at high injection concentrations, the high-energy sites become saturated by a few mobile-phase lysozyme molecules and then have little influence on the average retention volume. The retention volume at high injection concentrations is then dominated by interactions between the mobile-phase protein and low-energy sites, presumed to be isolated immobile protein molecules. However, examining the surface in Figure 5 at 33% surface coverage and considering the typical range of a protein−protein potential of mean force, a mobile lysozyme molecule is very likely to experience multibody interactions with immobilized lysozyme molecules. At high injection concentrations, all of the multibody sites are unlikely to be saturated by mobile protein molecules; there are very few "sites" where a mobile molecule can interact with a single immobile molecule. Discrepancies between chromatographically determined B_{22} values reported by Tessier et al. and those from static light scattering are consistent with the effect of multibody interactions in the chromatographic experiments: at low ionic strengths, B_{22} from chromatography is often more repulsive than that from static light scattering; at higher ionic strengths, the chromatographically determined values show much more attraction than those determined by static light scattering. These trends are especially apparent in Tessier's results with sodium chloride. Regrettably, Tessier et al. report only measurements up to moderate ionic strengths (~0.5 M). Our results show that, for

lysozyme, at higher ionic strengths, the discrepancy between static light scattering and chromatographic data is much more apparent.

Tessier et al. also studied chymotrysinogen self-interactions using chromatography. For chymotrypsinogen, Tessier et al. did not encounter the same problem; concentration-independent retention volumes were obtained in the low injection concentration limit. Chymotrypsinogen self-interactions are so weak that it is not possible to see effects of multibody interactions.

Our study reinforces the idea that working in the linear region of the isotherm does not guarantee that observed interactions are restricted to two-body interactions. That restriction can only be achieved by working at very low surface coverage.

Conclusions

We have used a chromatographic method to measure lysozyme−lysozyme interactions at a variety of solution conditions. To attain semiquantitative agreement with osmotic second virial coefficients from light scattering measurements, it was necessary to account for interactions between one mobile lysozyme particle and multiple immobile lysozyme particles. Our experimental data show that if chromatographic results are to yield meaningful osmotic second virial coefficients, chromatographic data must be interpreted very carefully. Obtaining data in the linear region of the isotherm is not sufficient to ensure that measured results correspond only to two-body protein−protein interactions. To obtain data for such two-body interactions, it is necessary that the immobile proteins be separated by a much larger distance than the effective range of the protein−protein potential.

Acknowledgment. We are grateful to the Office for Basic Sciences of the U.S. Department of Energy and to the National Science Foundation for financial support and to Alan Gilbert for assistance in data acquisition.

References and Notes

(1) Lomakin, A.; Teplow, D. B.; Kirschner, D. A.; Benedek, G. B. *Proc. Natl. Acad. Sci. U.S.A.* **1997**, *94*, 7942−7947.

(2) Conway, K. A.; Harper, J. D.; Lansbury, P. T. *Biochemistry* **2000**, *39*, 2552−2563.

(3) Heiser, V.; Scherzinger, E.; Boeddrich, A.; Nordhoff, E.; Lurz, R.; Schugardt, N.; Lehrach, H.; Wanker, E. E. *Proc. Natl. Acad. Sci. U.S.A.* **2000**, *97*, 6739−6744.

(4) Arnold, F.; Schofield, S.; Blanch, H. *J. Chromatogr.* **1986**, *355*, 1−12.

(5) Patro, S. Y.; Przybycien, T. M. *Biotechnol. Bioeng.* **1996**, *52*, 193−203.

(6) Zopf, D.; Ohlson, S. *Nature* **1990**, *346*, 87−88.

(7) Schittny, J. C. *Anal. Biochem.* **1994**, *222*, 140−148.

(8) Dunn, B. M. *Appl. Biochem. Biotechnol.* **1984**, *9*, 261−284.

(9) Tessier, P. M.; Lenhoff, A. M.; Sandler, S. I. *Biophys. J.* **2002**, *82*, 1620−1631.

(10) Rosenbaum, D. F.; Zukoski, C. F. *J. Cryst. Growth* **1996**, *169*, 752−758.

(11) Velev, O. D.; Kaler, E. W.; Lenhoff, A. M. *Biophys. J.* **1998**, *75*, 2682−2697.

(12) Curtis, R. A.; Ulrich, J.; Montaser, A.; Prausnitz, J. M.; Blanch, H. W. *Biotechnol. Bioeng.* **2002**, *79*, 367−380.

(13) Radke, C. J.; Prausnitz, J. M. *J. Chem. Phys.* **1972**, *57*, 714−722.

(14) Stahlberg, J.; Jonsson, B.; Horvath, C. *Anal. Chem.* **1991**, *63*, 1867−1874.

(15) McMillan, W.; Mayer, J. *J. Chem. Phys.* **1945**, *13*, 276−305.

(16) Grigsby, J. J.; Blanch, H. W.; Prausnitz, J. M. *Biophys. Chem.* **2001**, *91*, 231−243.

(17) tenWolde, P. R.; Frenkel, D. *Science* **1997**, *277*, 1975−1978.

(18) Feder, J. *J. Theor. Biol.* **1980**, *87*, 237−254.

(19) Domen, P. L.; Nevens, J. R.; Mallia, A. K.; Hermanson, G. T.; Klenk, D. C. *J. Chromatogr.* **1990**, *510*, 293−302.

(20) Sophianopoulus, A.; Rhodes, C.; Holcomb, D.; van Holde, K. *J. Biol. Chem.* **1962**, *237*, 1107−1112.

(21) Blanch, H. W.; Clark, D. S. *Biochemical Engineering*; Marcel Dekker: New York, 1996.

(22) DePhillips, P.; Lenhoff, A. M. *J. Chromatogr., A* **2000**, *883*, 39−54.

(23) Hagel, L.; Ostberg, M.; Andersson, T. *J. Chromatogr., A* **1996**, *743*, 33−42.

(24) Wang, Q.; Danwanichakul, P.; Glandt, E. D. *J. Chem. Phys.* **2000**, *112*, 6733−6738.

(25) Zhdanov, V. P.; Kasemo, B. *Proteins: Struct., Funct., Genet.* **2000**, *40*, 539−542.

(26) Kuehner, D. E.; Prausnitz, J. M.; Fergg, F.; Wernick, M.; Blanch, H. W.; Engmann, J. *J. Phys. Chem. B* **1999**, *103*, 1368−1374.

(27) Allen, M.; Tildesley, D. *Computer Simulation of Liquids*; Oxford University Press: New York, 1987.

(28) Ljunglof, A.; Larsson, M.; Knuuttila, K. G.; Lindgren, J. *J. Chromatogr., A* **2000**, *893*, 235−244.

(29) Hubbuch, J.; Linden, T.; Knieps, E.; Thommes, J.; Kula, M. R. *Biotechnol. Bioeng.* **2002**, *80*, 359−368.